Synthesis and Self-Organization of Core-Extended Perylene Tetracarboxdiimides with Branched Alkyl Substituents

Fabian Nolde, Wojciech Pisula, Sibylle Müller, Christopher Kohl, and Klaus Müllen*

Max-Planck-Institute for Polymer Research, Ackermannweg 10, D-55128 Mainz, Germany

Received March 29, 2006. Revised Manuscript Received June 6, 2006

The influence of the core extension of perylene tetracarboxdiimides on the thermotropic behavior has been investigated. A homologous series of alkyl substituted tetracarboxdiimides, namely, perylene diimide, terrylene diimide, quaterrylene diimide, and coronene diimide, was synthesized. These compounds display absorption maxima in the region of 430−760 nm with high extinction coefficients and show a high thermal stability up to 450 °C. Structural evaluation revealed an identical columnar self-organization for the derivatives below their isotropization temperature. An intracolumnar packing of the disks with a lateral rotation of 45° to each other resulted in a helical pitch containing four molecules. The phase transition to the isotropic phase is shifted to higher temperatures for larger aromatic cores within this series of compounds. On the other hand, differences in the self-assembly during crystallization from the isotropic phase were observed. While perylene tetracarboxdiimide and terrylene tetracarboxdiimide formed large and highly ordered domains with arranged edge-on molecules, the coronene tetracarboxdiimide disks self-organized face-on leading to a homeotropic phase. The different molecular orientation on surfaces was correlated with diversified substitution patterns of the aromatic cores. The manipulation of the molecular architecture opens thus the opportunity to control the spontaneous self-alignment. This improvement of the macroscopic organization ensures an undisturbed percolation pathway for charge carriers between electrodes in field-effect transistors or in photovoltaic cells.

Introduction

The development of organic semiconductors for electronic devices such as field-effect transistors[1] or photovoltaics[2] is a challenging topic of current research. Discotic liquid crystals, consisting of a rigid, disc-shaped aromatic core and disordered alkyl or alkoxy substituents, are promising materials in this field as they tend to self-organize in columnar supramolecular structures due to strong interactions between the aromatic cores and nanophase separation.[3] This $\pi-\pi$ overlap leads to energy bands comparable to those in inorganic semiconductors so that pronounced and defect-free, long-range ordered structures of these mesogens facilitate high charge carrier mobility along the columnar axis between the electrodes of a device.[4] Relationships between the chemical structure and the charge carrier mobility have been ascertained, showing that an effective intermolecular π overlap leads to an increase in the charge carrier mobility.[5−7] Large aryl cores such as hexa-*peri*-hexabenzocoronenes (HBC) exhibit high mobilities as a result of the large $\pi-\pi$ overlap integral.[8] The alkyl chains in the periphery allow the solubility in organic solvents to be controlled and the isotropization temperature of the liquid crystalline phase to be adjusted over a broader temperature range,[9,10] both of which are essential for facile processing.[10−15] In recent years, self-organization of liquid crystalline perylene tetracarboxdiimides (PDIs) have increasingly gained attention because of the opportunities presented by the combination of their liquid crystalline, photophysical, semiconducting, and photoconducting properties.[16−21] PDIs in general have been widely used as dyes and pigments because of their brilliant

* Corresponding author. Tel.: (+49) 6131 379 150. Fax: (+49) 6131 379 350. E-mail: muellen@mpip-mainz.mpg.de.

(1) Dimitrakopoulos, C. D.; Malenfant, P. R. L. *Adv. Mater.* **2002**, *14* (2), 99.
(2) Brabec, C. J.; Sariciftci, N. S.; Hummelen, J. C. *Adv. Mater.* **2001**, *11* (1), 15.
(3) Demus, D.; Goodby, J.; Gray, G. W.; Spiess, H.-W.; Vill, V. *Handbook of Liquid Crystals, Vol. 2B: Low Molecular Weight Liquid Crystals II*; Wiley-VCH: Weinheim, 1998.
(4) Lemeur, V.; da Silva Filho, D. A.; Coropceanu, V.; Lehmann, M.; Geerts, Y.; Piris, J.; Debije, M. G.; van de Craats, A. M.; Senthilkumar, K.; Siebbeles, L. D. A.; Warman, J. M.; Brédas, J.-L.; Cornil, J. *J. Am. Chem. Soc.* **2004**, *126*, 3271.
(5) van de Craats, A. M.; Warman, J. M. *Adv. Mater.* **2001**, *13*, 130.
(6) Pisula, W.; Tomovic, Z.; Simpson, C.; Kastler, M.; Pakula, T.; Müllen, K. *Chem. Mater.* **2005**, *17*, 4296.
(7) Chen, Z.; Debije, M. G.; Debaerdemaeker, T.; Osswald, P.; Würthner, F. *ChemPhysChem* **2004**, *5*, 137.
(8) van de Craats, A. M.; Warman, J. M.; Fechtenkötter, A.; Brand, J. D.; Harbison, M. A.; Müllen, K. *Adv. Mater.* **1999**, *11*, 1469.
(9) Kastler, M.; Pisula, W.; Wasserfallen, D.; Pakula, T.; Müllen, K. *J. Am. Chem. Soc.* **2005**, *127*, 4286.
(10) Pisula, W.; Kastler, M.; Wasserfallen, D.; Pakula, T.; Müllen, K. *J. Am. Chem. Soc.* **2004**, *126*, 8074.
(11) Pisula, W.; Tomovic, Z.; Stepputat, M.; Kolb, U.; Pakula, T.; Müllen, K. *Chem. Mater.* **2005**, *17*, 2641.
(12) Tracz, A.; Jeszka, J. K.; Watson, M. D.; Pisula, W.; Müllen, K.; Pakula, T. *J. Am. Chem. Soc.* **2003**, *125*, 1682.
(13) Pisula, W.; Menon, A.; Stepputat, M.; Lieberwirth, I.; Kolb, U.; Tracz, A.; Sirringhaus, H.; Pakula, T.; Müllen, K. *Adv. Mater.* **2005**, *17*, 684.
(14) van de Craats, A. M.; Stutzmann, N.; Bunk, O.; Nielsen, M. M.; Watson, M.; Müllen, K.; Chanzy, H. D.; Sirringhaus, H.; Friend, R. H. *Adv. Mater.* **2003**, *15*, 495.
(15) Piris, J.; Debije, M. G.; Stutzmann, N.; Laursen, B. W.; Pisula, W.; Watson, M. D.; Bjornholm, T.; Müllen, K.; Warman, J. M. *Adv. Funct. Mater.* **2004**, *14*, 1053.
(16) Würthner, F. *Chem. Commun.* **2004**, 1564.
(17) Cormier, R. A.; Gregg, B. A. *Chem. Mater.* **1998**, *10*, 1309.
(18) Iverson, I. K.; Tam-Chang, S.-W. *J. Am. Chem. Soc.* **1999**, *121*, 5801.
(19) Gregg, B. A.; Cormier, R. A. *J. Am. Chem. Soc.* **2001**, *123*, 7959.

10.1021/cm060742c CCC: $33.50
Published on Web 07/15/2006

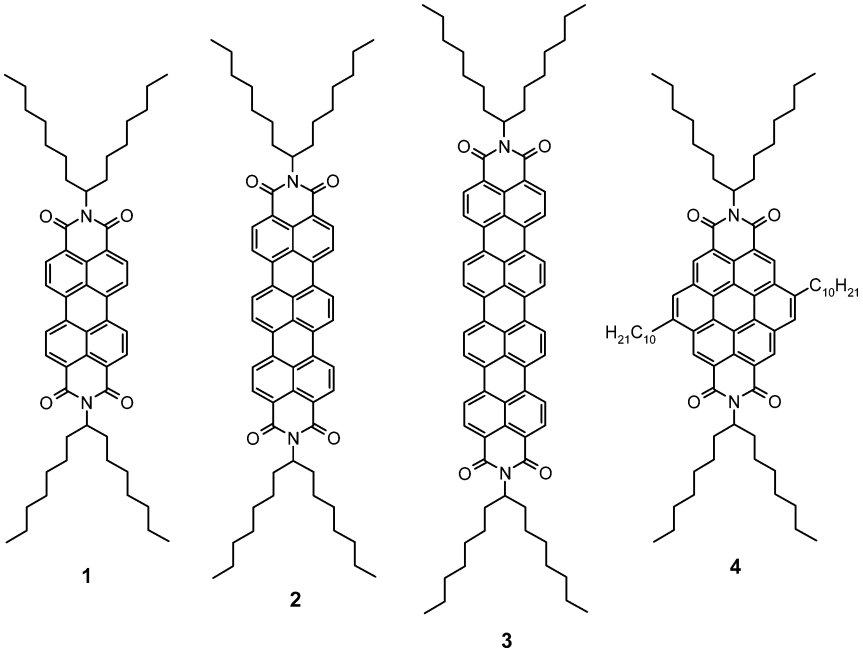

Figure 1. Rylenes (**1**−**3**) and CDI (**4**).

orange and red colors. In addition, their high extinction coefficients and high thermal, chemical, and photochemical stabilities make them suitable as functional dyes in electronic devices.[22] The higher homologues of PDIs, namely, terrylene and quaterrylene tetracarboxdiimides (TDIs and QDIs),[23,24] exhibit the same attractive properties. Their absorption maximum is bathochromically shifted to 600 and 800 nm so that this series of rylene dyes covers practically the visible light and the near-infrared region.

For organic field-effect transistors (OFETs), a number of electron-rich aromatic systems that are good hole transporting materials (p-type materials) have been discovered, including pentacene which is the current benchmark organic semiconductor for OFETs.[25] n-Type organic semiconductors of high mobility for electron transport, which are also desired because they will enable the fabrication of complimentary circuits, have been found only in limited number.[26] In the liquid crystalline phase forming *N*,*N*′-alkylperylene tetracarboxdiimide the majority of the charge carriers are electrons, and these PDIs are thus classified as n-type materials. Mobilities up to 0.6 $cm^2\ V^{-1}\ s^{-1}$ and current on/off ratios $>10^5$ were obtained for thin-film transistors based on *N*,*N*′-dioctyl-3,4:9,10-perylene tetracarboxdicarboximide.[27,28] The use of perfluoroalkyl chains as imide substituents increased solubility and air stability in OFET operation.[29,30] Furthermore, these materials became promising as acceptor components for heterojunction photovoltaic devices.[31] A significant step toward organic thin film photovoltaic devices has been made with a combination of the liquid crystalline HBC and a PDI with branched alkyl chains.[32] Using a blending technique, these materials were allowed to self-assemble into a two-phase photovoltaic material which showed an extraordinary performance. With such photovoltaic cells, a quantum efficiency (the ratio of light absorbed to electrical energy produced) of 34% using 490 nm light was achieved. To increase the efficiency of organic solar cells, it is important to design rylene tetracarboxdiimide derivatives which exhibit a high degree of order in the bulk. As such, liquid crystalline perylene derivatives are promising candidates for organic solar cells.

The use of branched alkyl chains instead of *n*-alkyl chains on one hand and expanding the PDI core, either along the long molecular axis leading to the next higher homologous TDI and QDI or along the short axis as fulfilled in the coronene tetracarboxdiimides (CDIs) (Figure 1), on the other hand, should have advantages for their use in electronic devices: branched alkyl chains will increase solubility and lower the isotropization temperature of the liquid crystalline phase for better processing. Enlargement of the aromatic core is supposed to achieve a more effective $\pi-\pi$ interaction

(20) An, Z.; Yu, J.; Jones, S. C.; Barlow, S.; Yoo, S.; Domercq, B.; Prins, P.; Siebbeles, L. D. A.; Kippelen, B.; Marder, S. R. *Adv. Mater.* **2005**, *17* (21), 2580.
(21) Neuteboom, E. E.; Meskers, S. C. J.; Meijer, E. W.; Jannssen, R. A. J. *Macromol. Chem. Phys.* **2004**, *205*, 217.
(22) Zollinger, H. *Color Chemistry*; Wiley-VCH: Weinheim, 2003.
(23) Holtrup, F. O.; Müller, G. R. J.; Quante, H.; De Feyzer, S.; De Schryver, F. C.; Müllen, K. *Chem.—Eur. J.* **1997**, *3* (2), 219.
(24) Quante, H.; Müllen, K. *Angew. Chem., Int. Ed.* **1995**, *34*, 1323.
(25) Lin, Y.-Y.; Gundlach, D. J.; Nelson, S.; Jackson, T. N. *IEEE Electron Device Lett.* **1997**, *18*, 606.
(26) Chesterfield, R. J.; McKeen, J. C.; Newman, C. R.; Ewbank, P. C.; da Silva Filho, D. A.; Brédas, J.-L.; Miller, L. L.; Mann, K. R.; Frisbie, C. D. *J. Phys. Chem. B* **2004**, *108*, 19281.
(27) Struijk, W.; Sieval, A. B.; Dakhorst, J. E. J.; van Dijk, M.; Klimkes, P.; Koehorst, R. B. M.; Donker, H.; Schaafsma, T. J.; Picken, S. J.; van de Craats, A. M.; Warmann, J. M.; Zuilhof, H.; Sudhölter, E. J. R. *J. Am. Chem. Soc.* **2000**, *122*, 11027.
(28) Malenfant, P. R. L.; Dimitrakopoulos, C. D.; Gelorme, J. D.; Kosbar, L. L.; Graham, T. O.; Curioni, A.; Andreoni, W. *Appl. Phys. Lett.* **2002**, *80* (14), 2517.
(29) Jones, B. A.; Ahrens, M. J.; Yoon, M.-H.; Faccetti, A.; Marks, T. J.; Wasielewski, M. R. *Angew. Chem., Int. Ed.* **2004**, *43*, 6363.
(30) Facchetti, A.; Mushrush, M.; Katz, H. E.; Marks, T. J. *Adv. Mater.* **2003**, *15* (1), 33.
(31) Würthner, F.; Chen, Z. J.; Hoeben, F. J. M.; Osswald, P.; You, C. C.; Jonkheijm, P.; von Herrikhuyzen, J.; Schenning, A. P. H. J.; van der Schoot, P. P. A. M.; Meijer, E. W.; Beckers, E. H. A.; Meskers, S. C. J.; Janssen, R. A. J. *J. Am. Chem. Soc.* **2004**, *126*, 10611.
(32) Schmidt-Mende, L.; Fechtenkötter, A.; Müllen, K.; Moons, E.; Friend, R. H.; MacKenzie, J. D. *Science* **2001**, *293*, 1119.

leading to highly ordered supramolecular architectures and higher charge carrier mobilities.

Within the rylene tetracarboxdiimide series a higher charge carrier mobility has been observed for *N*,*N*′-dioctylperylene tetracarboxdiimide than for the respective *N*,*N*′-dioctylnaphthalene tetracarboxdiimide.[33,34] However, there is no report of a systematic investigation of the liquid crystalline behavior which includes the higher homologues, TDI and QDI. The self-organization of these compounds has not been investigated thus far. The phase forming behavior of CDIs is published but only *n*-alkyl or aryl imides are known so far.[35] Hence, to provide a fundamental understanding of the spontaneous self-assembly of core-extended perylene derivatives with branched alkyl chains from the isotropic phase, rylenes **1**−**3** and the coronene **4** were synthesized, and polarized optical microscopy (POM) as well as two-dimensional wide-angle X-ray scattering (2D-WAXS) experiments of extruded filaments were employed.

Experimental Section

General Details. Melting points were performed on a Büchi melting point apparatus and are not corrected. ^{1}H NMR and ^{13}C NMR spectra were recorded in deuterated solvents on Bruker Avanche 250, Bruker AMX 300, Bruker DRX 500, and Bruker Avance 700 instruments, using the residual proton resonance or the carbon signal of the solvent as the internal standard. For ^{13}C J-modulated spin−echo NMR measurements, the abbreviations q and t represent quaternary carbons, and CH_2, CH_3, CH groups, respectively. Infrared spectra were obtained on a Nicolet FT-IR 320 instrument. UV/vis spectra were recorded on a Perkin-Elmer Lambda 40 spectrophotometer at room temperature. Fluorescence spectra were recorded on a Spex Fluorolog 3 spectrometer. FD (Field Desorption) mass spectra were obtained on a VG Instruments ZAB 2-SE-FPD. 1,7-Dibromo-3,4:9,10-perylene tetracarboxdianhydride was provided by the BASF AG. All other starting materials were purchased from Aldrich, Acros, ABCR, or Lancaster and used as received.

Differential scanning calorimetry (DSC) was measured on a Mettler DSC 30 with heating and cooling rates of 10 K/min. The 2D-WAXS experiments were performed by means of a rotating anode (Rigaku 18 kW) X-ray beam with a pinhole collimation and a two-dimensional Siemens detector. A double graphite monochromator for the Cu Kα radiation ($\lambda = 0.154$ nm) was used. A Zeiss microscope equipped with polarizing filters and equipped with a Hitachi KP-D50 color digital charge-coupled device camera was used to investigate the optical textures of the compounds. The samples were sandwiched between two glass slides and then thermally treated on a Linkam hotstage fitted with a Linkam TMS 91 temperature controller.

Synthesis. *N-(1-Heptyloctyl)-4-bromonaphthalene-1,8-dicarboxmonoimide (**10**).* A total of 5 g (18 mmol) of 4-bromonaphthalene-1,8-dicarboxmonoimide (**9**) was heated with 6.1 g (27 mmol) of 1-heptyloctylamine in 50 mL of ethylene glycol at 160 °C for 4 h. The resulting solution was cooled to room temperature and diluted with 50 mL of methanol and 50 mL of distilled water. The crude product was extracted with diethyl ether, the solution was dried over $MgSO_4$, and the solvent was evaporated. The remaining yellow oil was further purified by column chromatography with dichloromethane as the eluent to afford 5.5 g (63%) of the title compound as a colorless oil. ^{1}H NMR (300 MHz, $C_2D_2Cl_4$, 25 °C): δ 8.53 (m, 1H), 8.44 (d, 1H, $J = 8.5$ Hz), 8.29 (m, 1H), 7.95 (d, 1H, $J = 7.9$ Hz), 7.76 (t, 1H, $J = 7.6$ Hz), 5.08−4.96 (m, 1H), 2.15−2.06 (m, 2H), 1.77−1.70 (m, 2H), 1.17−1.10 (m, 20 H), 0.77−0.72 (m, 6H). ^{13}C NMR (75 MHz, $C_2D_2Cl_4$, 25 °C): δ 165.02, 163.88, 133.19, 132.67, 131.38, 131.22, 130.69, 130.21, 129.35, 128.41, 123.98, 123.25, 123.12, 122.39, 54.91, 32.57, 32.15, 29.57, 27.22, 22.98, 14.50. IR (NaCl) υ (cm $^{-1}$): 2924, 2854, 2362, 1704, 1663, 1619, 1588, 1508, 1461, 1400, 1342, 1239, 783. MS (FD): [M^+] calcd for $C_{27}H_{36}NBrNO_2$, 486.50; found, 486.1 (100%).

*N-(1-Heptyloctyl)perylene-3,4-dicarboxmonoimide (**6**).* A total of 6 g (19 mmol) of perylene-3,4-dianhydride (**5**) was reacted with 10.7 g (47 mmol) of 1-heptyloctylamine in 100 mL of quinoline at 160 °C. After stirring the mixture under argon for 12 h the reaction was cooled to room temperature and diluted with hydrochloric acid. The precipitate was filtered and dried under vacuum. For further purification the crude product was chromatographed on silica gel with dichloromethane to afford 8.4 g (83%) of a red solid. Mp: 156 °C. ^{1}H NMR (250 MHz, $C_2D_2Cl_4$, 25 °C): δ 8.38 (m, 2H), 8.17 (d, 2H, $J = 7.9$ Hz), 8.12 (d, 2H, $J = 8.2$ Hz), 7.75 (d, 2H, $J = 7.9$ Hz), 7.47 (t, 2H, $J = 7.6$ Hz), 5.17−5.05 (m, 1H), 2.23−2.16 (m, 2H), 1.89−1.81 (m, 2H), 1.27−1.20 (m, 20H), 0.82−0.77 (m, 6H). ^{13}C NMR (62.5 MHz, $C_2D_2Cl_4$, 25 °C): δ 165.24, 164.24, 136.85, 134.22, 131.90, 131.20, 131.00, 129.83, 129.09, 127.79, 127.16, 126.53, 123.77, 121.61, 120.84, 120.21, 54.58, 32.65, 32.15, 29.91, 29.58, 27.39, 22.97, 14.50. IR (KBr) υ (cm $^{-1}$): 2924, 2853, 2365, 1697, 1653, 1594, 1572, 1450, 1460, 1408, 1355, 1292, 1244, 1172, 1136, 1109, 840, 754. UV−vis ($CHCl_3$) λ_{max} (ϵ): 511 (50 000), 489 nm (50 000 M^{-1} cm^{-1}). Fluorescence ($CHCl_3$) λ_{max}: 571, 544 nm. MS (FD): [M^+] calcd for $C_{37}H_{41}NO_2$, 531.74; found, 531.2 (100%).

*N-(1-Heptyloctyl)-9-bromoperylene-3,4-dicarboxmonoimide (**7**).* A total of 8 g (15.05 mmol) of *N*-(1-heptyloctyl)perylene-3,4-dicarboxmonoimide (**6**) was suspended for 0.5 h in 100 mL of acetic acid. After adding 150 mg (0.6 mmol) of iodine and 9.6 g (60.2 mmol) of bromine, the mixture was stirred for 4.5 h at room temperature under light exclusion. The excess of bromine was removed by bubbling argon into the flask, and the mixture was precipitated by 100 mL of methanol and stirred overnight. The product was filtrated and washed with 150 mL of methanol. Drying under vacuum afforded 8.9 g (97%) of the title compound. Mp: 163 °C. ^{1}H NMR (500 MHz, CD_2Cl_2, 25 °C): δ 8.63 (d, 1H, $J = 8.2$ Hz), 8.61 (d, 1H, $J = 8.2$ Hz), 8.45 (d, 1H, $J = 8.2$ Hz), 8.42 (d, 1H, $J = 8.2$ Hz), 8.36 (d, 1H, $J = 7.6$ Hz), 8.27 (d, 1H, $J = 8.2$ Hz), 8.20 (d, 1H, $J = 8.2$ Hz), 7.87 (d, 1H, $J = 8.2$ Hz), 7.70 (t, 1H, $J = 7.6$ Hz), 5.17−5.05 (m, 1H), 2.23−2.16 (m, 2H), 1.89−1.81 (m, 2H), 1.27−1.20 (m, 20 H), 0.82−0.77 (m, 6H). ^{13}C NMR (Spinecho, 125 MHz, CD_2Cl_2, 25 °C): δ 165.16, 164.12, 136.16, 132.73, 132.01, 131.26, 129.90, 129.73, 129.47, 128.93, 128.20, 126.14, 126.08, 124.38, 123.67, 122.06, 121.31, 120.75, 120.48, 54.69, 32.65, 32.15, 29.90, 29.59, 27.40, 22.98, 14.53. IR (KBr) υ (cm $^{-1}$): 2924, 2853, 2365, 1697, 1653, 1594, 1572, 1450, 1460, 1408, 1355, 1292, 1244, 1172, 1136, 1109, 840, 810, 754. UV−vis ($CHCl_3$) λ_{max} (ϵ): 514 (51 000), 489 nm (52 000 M^{-1} cm^{-1}). Fluorescence ($CHCl_3$) λ_{max}: 571, 544 nm. MS (FD): [M^+] calcd for $C_{37}H_{40}BrNO_2$, 610.64; found, 611.1 (100%).

*N-(1-Heptyloctyl)-9-(4,4,5,5-tetramethyl-1,3,2-dioxaborolan-2-yl)perylene-3,4-dicarboxmonoimide (**8**).* A total of 1.2 g (2 mmol) of *N*-(1-heptyloctyl)-9-bromoperylene-3,4-dicarboxmonoimide (**7**) and 558 mg (2.5 mmol) of bis(pinacolato)diboron were mixed together with 588 mg (5.3 mmol) of potassium acetate in 20 mL

(33) Katz, H. E.; Lovinger, A. J.; Johnson, J.; Kloc, C.; Siegrist, T.; Li, W.; Lin, Y.-Y.; Dodabalapur, A. *Nature (London)* **2000**, *404*, 478.
(34) Katz, H. E.; Johnson, J.; Lovinger, A. J.; Li, W. *J. Am. Chem. Soc.* **2000**, *122* (32), 7787.
(35) Rohr, U.; Kohl, C.; Müllen, K.; van de Craats, A.; Warman, J. *J. Mater. Chem.* **2001**, *11*, 1789.

of dioxane under a light stream of argon. Finally 44 mg (0.1 mmol) of [$PdCl_2$(dppf)] × CH_2Cl_2 was added, and the reaction mixture was stirred under argon atmosphere for 16 h at 70 °C. After cooling to room temperature, the mixture was extracted with dichloromethane and washed twice with distilled water. The dichloromethane layer was separated and dried over $MgSO_4$, and the crude product was purified by column chromatography with dichloromethane as the eluent to afford 1.0 g (78%) of the product as a red solid. Mp: 213 °C. ^{1}H NMR (300 MHz, THF-d_8, 25 °C): δ 8.87 (d, 1H, J = 7.7 Hz), 8.55−8.47 (m, 6H), 8.15 (d, 1H, J = 7.7 Hz), 7.59 (t, 1H, J = 7.7 Hz), 5.27−5.17 (m, 1 H), 2.40−2.28 (m, 2H), 1.84−1.77 (m, 2H), 1.44 (s, 12H), 1.34−1.24 (m, 20H), 0.85−0.81 (t, 6H, J = 6.8 Hz). ^{13}C NMR (75 MHz, THF-d_8, 25 °C): δ 165.24, 164.33, 139.04, 137.83, 137.28, 132.81, 132.20, 131.45, 130.64, 130.02, 128.60, 127.81, 127.40, 124.38, 123.34, 123.25, 122.04, 121.90, 121.28. IR (KBr) υ (cm $^{-1}$): 2925, 2854, 2362, 2337, 1691, 1653, 1592, 1507, 1461, 1416, 1376, 1332, 1272, 1246, 1209, 1142, 1113, 1068, 966, 858, 811, 754, 674. UV−vis ($CHCl_3$) λ_{max} (ϵ): 514 (47 000), 489 nm (45 000 M^{-1} cm^{-1}). Fluorescence ($CHCl_3$) λ_{max}: 577, 546 nm. MS (FD): [M^+] calcd for $C_{43}H_{52B}N_2O_4$, 657.71; found, 657.2 (100%).

*N-(1-Heptyloctyl)-9-(4-N-(1-heptyloctyl)naphthalene-1,8-dicarboximide)perylene-3,4-dicarboxmonoimide (**11**).* *N*-(1-Heptyloctyl)-9-(4,4,5,5-tetramethyl-1,3,2-dioxaborolan-2-yl)perylene-3,4-dicarboxmonoimide (**8**; 1.0 g, 1.52 mmol) and *N*-(1-heptyloctyl)-4-bromonaphthalene-1,8-dicarboxmonoimide (**10**; 0.813 g, 1.67 mmol) were dissolved in toluene (76 mL). A solution of Na_2CO_3 in water (63 mL, 1 M) and ethanol (5 mL) was added, and the mixture was flushed with argon. [$Pd(PPh_3)_4$] catalyst (80 mg, 0.06 mmol) was added, and the reaction mixture was stirred under argon for 16 h at 80 °C. The reaction mixture was cooled to room temperature. The organic phase was separated, and the solvent was evaporated under reduced pressure. For further purification the crude product was chromatographed on silica gel with dichloromethane to afford 1.1 g (79%) of a red solid. Mp: 129 °C. ^{1}H NMR (700 MHz, $C_2D_2Cl_4$, 130 °C) δ 8.68 (d, 1H, J = 6.7 Hz), 8.64−8.56 (m, 3H), 8.53 (d, 1H), 8.47 (d, 1H), 8.45−8.39 (m, 2H), 7.85−7.75 (m, 2H), 7.62 (d, 1H, J = 6.8 Hz), 7.59−7.54 (m, 1H), 7.45 (d, 1H, J = 7.1 Hz), 7.41 (d, 1H, J = 7.8 Hz), 5.22−5.11 (m, 2H), 2.31−2.19 (m, 4H), 1.98−1.86 (m, 4H), 1.41−1.19 (m, 40H), 0.93−0.77 (m, 12H). ^{13}C NMR (175 MHz, $C_2D_2Cl_4$, 130 °C): δ 164.77, 164.63, 164.53, 144.02, 139.39, 136.84, 136.57, 133.87, 131.96, 131.64, 131.60, 131.36, 131.33, 130.58, 130.51, 130.27, 130.24, 129.32, 129.09, 129.03, 127.71, 127.32, 127.06, 124.18, 123.91, 123.83, 122.94, 122.64, 122.50, 120.89, 120.80, 55.16, 55.00, 32.93, 32.90, 31.93, 31.90, 29.64, 29.24, 27.24, 22.61, 13.92. IR (KBr) υ (cm $^{-1}$): 2956, 2927, 2850, 1697, 1654, 1590, 1577, 1348, 811. UV−vis ($CHCl_3$) λ_{max} (ϵ): 508 (40 000), 482 (39 000), 350 (14 000), 335 nm (16 000 M^{-1} cm^{-1}). MS (FD): [M^+] calcd for $C_{64}H_{76}N_2O_4$, 937.33; found, 937.5 (100%).

*N,N′-Di(1-heptyloctyl)terrylene-3,4:11,12-tetracarboxdiimide (**2**).* *N*-(1-Heptyloctyl)-9-(4-*N*-(1-heptyloctyl)naphthalene-1,8-dicarboxmonoimide)perylene-3,4-dicarboxmonoimide (**11**; 0.9 g, 0.96 mmol), K_2CO_3 (6.42 g, 46.5 mmol), and ethanolamine (9.0 g, 0.147 mol) were stirred under argon for 3 h at 160 °C. After cooling to room temperature the solution was poured into methanol (20 mL). The precipitate was filtered, washed with water, dried under vacuum, and purified by column chromatography on silica gel (CH_2Cl_2) to yield the blue product (0.763 g, 85%). Mp: 278 °C. ^{1}H NMR (250 MHz, THF-d_8, 25 °C): δ 8.25 (s, 4H), 8.18 (d, 8H, J = 8.5 Hz), 5.21 (m, 2H), 2.37 (m, 4H, J = 6.95 Hz), 1.92 (m, 4H), 1.42−1.30 (m, 40H), 0.89−0.84 (m, 12 H). ^{13}C NMR (125 MHz, THF-d_8, 25 °C): δ 164.43, 163.52, 135.18, 130.52, 129.77, 127.85, 125.76, 124.35, 122.90, 122.04, 121.34, 54.78, 33.20, 32.79, 30.51, 30.17, 28.06, 23.43, 14.34. IR (KBr) υ (cm $^{-1}$): 2923, 2852, 1694, 1652, 1585, 1379, 1353, 1323, 807. UV−vis ($CHCl_3$) λ_{max} (ϵ): 651 (127 000), 598 (66 000), 547 nm (21 000 M^{-1} cm^{-1}). Fluorescence ($CHCl_3$) λ_{max}: 669, 729 nm. MS (FD): [M^+] calcd for $C_{64}H_{74}N_2O_4$, 935.31; found, 935.6 (100%).

*N,N′-Bis(1-heptyloctyl)-9,9′-biperylene-3,4:3′,4′-bis(dicarboxmonoimide) (**12**).* *N*-(1-Heptyloctyl)-9-(4,4,5,5-tetramethyl-1,3,2-dioxaborolan-2-yl)perylene-3,4-dicarboxmonoimide (**8**; 0,2 g, 0,3 mmol) and *N*-(1-heptyloctyl)-9-bromoperylene-3,4-dicarboxmonoimide (**7**; 0.37 g, 0.6 mmol) were dissolved in toluene (15 mL). A solution of Na_2CO_3 in water (10 mL, 1 M) and ethanol (5 mL) was added, and the mixture was flushed with argon. [$Pd(PPh_3)_4$] catalyst (16 mg, 0.01 mmol) was added, and the reaction mixture was stirred under argon for 16 h at 80 °C. The reaction mixture was cooled to room temperature. The organic phase was separated, and the solvent was evaporated under reduced pressure. For further purification the crude product was chromatographed on silica gel with dichloromethane to afford 0.24 g (76%) of a red solid. Mp: 304 °C. ^{1}H NMR (700 MHz, $C_2D_2Cl_4$, 130 °C): δ 8.65−8.57 (m, 4H), 8.54 (d, 2H, J = 7.4 Hz), 8.47 (d, 2H, J = 7.7 Hz), 8.45−8.40 (m, 4H), 7.68 (d, 2H, J = 7.3 Hz), 7.55 (d, 2H, J = 8.0 Hz), 7.46 (t, 2H, J = 8.0 Hz), 5.22−5.11 (m, 2H), 2.30−2.19 (m, 4H), 1.97−1.85 (m, 4H), 1.37−1.19 (m, 40H), 0.94−0.780 84 (m, 12H). ^{13}C NMR (75 MHz, $C_2D_2Cl_4$, 130 °C): δ 164.58, 140.68, 137.01, 136.80, 134.15, 131.63, 130.29, 130.19, 130.10, 129.45, 129.24, 128.83, 127.56, 127.08, 123.88, 123.18, 122.46, 122.39, 120.77, 120.65, 54.99, 32.91, 31.91, 29.66, 29.26, 27.26, 22.62, 13.93. IR (KBr) υ (cm $^{-1}$): 2954, 2925, 2854, 1693, 1653, 1593, 1572, 1352, 812. UV−vis ($CHCl_3$) λ_{max} (ϵ): 527 nm (97 000 M^{-1} cm^{-1}). MS (FD): [M^+] calcd for $C_{74}H_{80}N_2O_4$, 1061.47; found,1060.0 (100%).

*N,N′-Di(1-heptyloctyl)quaterrylene-3,4:13,14-tetracarboxdiimide (**3**).* *N,N′*-Bis(1-heptyloctyl)-9,9′-biperylene-3,4:3′,4′-bis(dicarboximide) (**12**; 0.2 g, 0.19 mmol), K_2CO_3 (1.26 g, 9.1 mmol), and ethanolamine (1.7 g, 0.028 mol) were stirred under argon for 3 h at 160 °C. After cooling to room temperature the solution was poured into methanol (10 mL). The precipitate was filtered, washed with water, dried under vacuum, and purified by column chromatography on silica gel (CH_2Cl_2) to yield the blue green product (0.165 g, 83%). Mp: >350 °C. ^{1}H NMR (300 MHz, $C_2D_2Cl_4$, 120 °C): δ 8.47 (m, 16H), 5.17 (m, 2H), 2.25 (m, 4H), 1.93 (m, 4H), 1.32 (m, 40H), 0.84 (m, 12H). ^{13}C NMR (75 MHz, THF-d_8, 25 °C): δ 164.14, 163.79, 140.81, 135.80, 131.51, 130.38, 129.34, 127.99, 127.17, 126.34, 124.15, 123.21, 120.68, 55.03, 33.51, 33.03, 30.81, 30.43, 28.38, 23.65, 14.56. IR (KBr) υ (cm $^{-1}$): 2956, 2925, 2856, 1693, 1652, 1575, 1349, 1286, 809. UV−vis ($CHCl_3$) λ_{max} (ϵ): 762 nm (162 000 M^{-1} cm^{-1}). MS (FD): [M^+] calcd for $C_{74}H_{78}N_2O_4$, 1059.4; found, 1058.1 (100%).

*N,N′-Bis(1-heptyloctyl)-1,7-dibromoperylene-3,4:9,10-tetracarboxdiimide (**14**).* 1,7-Dibromoperylene-3,4:9,10-tertacarboxdianhydride (**13**; 0.5 g, 0.909 mmol and 1-heptyloctylamine (0.75 g, 3.298 mmol) were stirred in 50 mL of *N*-methylpyrrolidone (NMP) for 4 h at 150 °C. After cooling to room temperature the solution was poured into diluted hydrochloric acid (400 mL). The precipitate was filtered, washed with water and methanol, dried under vacuum, and purified by column chromatography on silica gel (petrol ether/CH_2Cl_2, 3:2) to yield the red product (0.34 g, 39%). ^{1}H NMR (300 MHz, CD_2Cl_2, 25 °C): δ 9.53 (s, 1H), 9.50 (s, 1H), 8.89 (sb, 2H), 8.66 (dd, J = 7.2 Hz, 2H), 5.20−5.12 (m, 2H), 2.25−2.20 (m, 4H), 1.86−1.80 (m, 4H), 1.28−1.22 (m, 40H), 0.85−0.81 (m, 12H). ^{13}C NMR (75 MHz, CD_2Cl_2, 25 °C): δ 162.55 (C═O), 138.21, 137.13, 132.86, 132.66, 131.52, 130.10, 129.28, 128.48, 127.18, 120.61, 54.75, 41.08, 31.77, 29.44, 29.18, 26.85, 22.59, 13.79. IR (KBr) υ (cm $^{-1}$): 2956, 2925, 2854, 1703, 1660, 1589, 1381, 1329, 1240, 810, 748. UV−vis ($CHCl_3$) λ_{max} (ϵ): 390 (6000), 460

Scheme 1. Synthesis of 2 and 3[a]

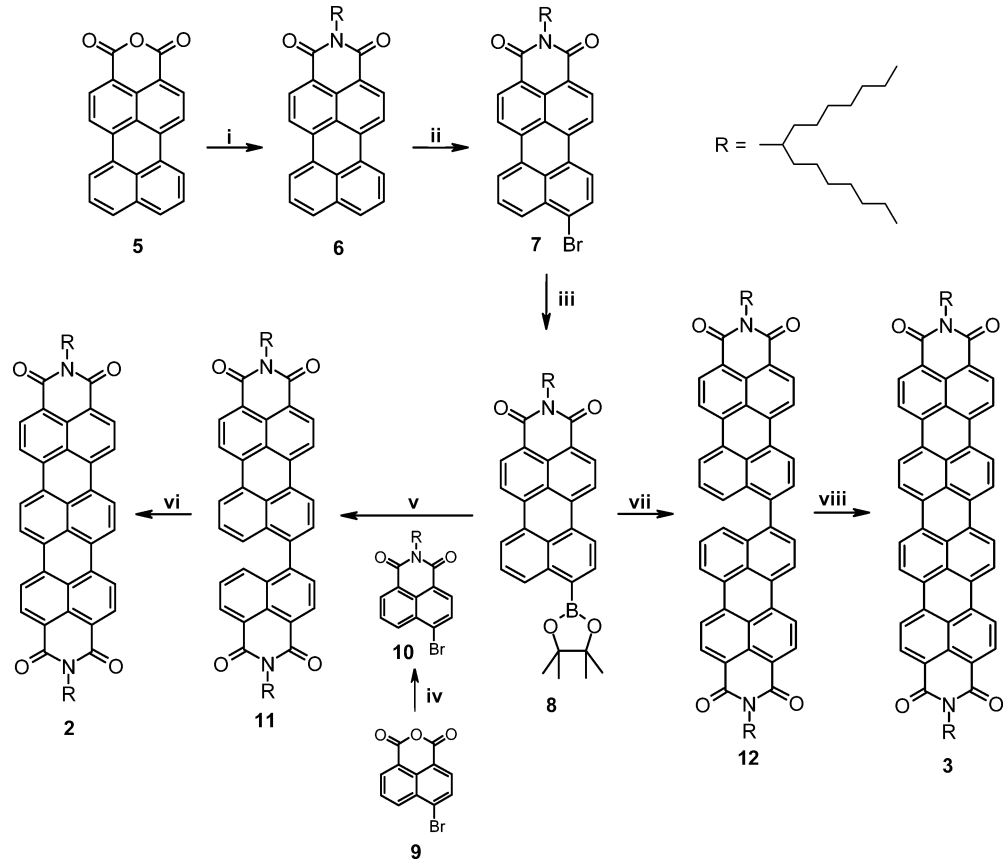

[a] (i) 1-Heptyloctylamine, quinoline, 160 °C, 12 h, 83%; (ii) Br_2, I_2, acetic acid, reflux, 4.5 h, 97%; (iii) [$PdCl_2$(dppf)] × CH_2Cl_2, bis(pinacolato)diboron, dioxane, 70 °C, 16 h, 78%; (iv) 1-heptyloctylamine, ethylene glycol, 160 °C, 4 h, 63%; (v) [$Pd(PPh_3)_4$], Na_2CO_3/H_2O, toluene, 80 °C, 16 h, 79%; (vi) ethanolamine, K_2CO_3, 160 °C, 3 h, 85%; (vii) [$Pd(PPh_3)_4$], Na_2CO_3/H_2O, toluene, 80 °C, 16 h, 76%; and (viii) ethanolamine, K_2CO_3, 160 °C, 3 H, 83%.

(15 000), 490 (37 000), 526 nm (55 000 M^{-1} cm^{-1}). MS (FD): [M^+] calcd for $C_{54}H_{68}Br_2N_2O_4$, 968.96; found, 971.3 (100%).

*N,N′-Bis(1-heptyloctyl)-1,7-didocen-1-yneperylene-3,4:9,10-tetracarboxdiimide (**15**).* *N,N′*-Bis(1-heptyloctyl)-1,7-dibromoperylene-3,4:9,10-tetracarboxdiimide (**14**; 0.2 g, 0.206 mmol), dodec-1-yne (0.14 g, 0.824 mmol), [$Pd(PPh_3)_2Cl_2$] (25 mg, 0.021 mmol), triphenylphosphine (6 mg, 0.020 mmol), and copper iodide (4 mg, 0.020 mmol) were stirred in a mixture of 20 mL of triethylamine and 20 mL of tetrahydrofuran (THF) for 16 h at 80 °C. After cooling to room temperature the solution was poured into dilute HCl (100 mL), and the mixture was extracted with CH_2Cl_2. The solvent was evaporated under reduced pressure, and the resulting solid was purified by column chromatography on silica gel (pentane/CH_2Cl_2, 3:1) to yield the red product (0.15 g, 64%). The product contains small amounts of the cyclized product **4**, which can be separated by a very careful column chromatography on silica gel (pentane/CH_2Cl_2, 3:1). ^{1}H NMR (300 MHz, $C_2D_2Cl_4$, 100 °C): δ 10.13 (d, J = 8.2 Hz, 2H), 8.72 (s, 2H), 8.60 (d, J = 8.2 Hz, 2H), 5.12 (sept, J = 6.1 Hz, 2H), 2.63 (t, J = 7.1 Hz, 4H), 2.22−2.17 (m, 4H), 1.89−1.74 (m, 8H), 1.58−1.53 (m, 4H), 1.26−1.22 (m, 64H), 0.84−0.79 (m, 18H). ^{13}C NMR (75 MHz, $C_2D_2Cl_4$, 100 °C, spin−echo experiment): δ 164.11 (C═O), 138.34 (t), 134.44 (q), 134.00 (q), 130.49 (t), 127.97 (q), 127.85 (q), 127.18 (t), 123.66 (q), 122.71 (q), 121.28 (q), 102.06 (q), 82.82 (q), 55.18 (CH), 32.77 (CH_2), 32.03 (CH_2), 31.96 (CH_2), 29.73 (CH_2), 29.67 (CH_2), 29.43 (CH_2), 29.40 (CH_2), 29.33 (CH_2), 29.29 (CH_2), 28.61 (CH_2), 27.19 (CH_2), 22.76 (CH_2), 22.70 (CH_2), 20.52 (CH_2), 14.12 (CH_3), 14.09 (CH_3). IR (KBr) υ (cm^{-1}): 2958, 2925, 2856, 2214, 1699, 1657, 1601, 1589, 1466, 1410, 1342, 1327, 1259, 1246, 812, 756, 706. UV−vis ($CHCl_3$) λ_{max} (ϵ): 413 (7000), 477 (13 000), 512 (28 000), 553 nm (48 000 M^{-1} cm^{-1}). MS (FD): [M^+] calcd for $C_{78}H_{110}N_2O_4$, 1139.76; found, 1139.7 (100%).

*N,N′-Di(1-heptyloctyl)-5,11-didecylcoronene-2,3:8,9-tetracarboxdiimide (**4**).* *N,N′*-Di(1-heptyloctyl)-1,7-di(dodec-1-ynyl)perylen-3,4:9,10-tetracarboxydiimide (**15**; 0.1 g, 0.088 mmol) were dissolved in 30 mL of toluene, and the solution was deoxygenated with argon. 1,8-Diazabicyclo[5.4.0]undec-7-ene (DBU; 0.1 mL) was added, and the mixture was stirred for 20 h at 110 °C. After cooling to room temperature, the solution was poured into ice cold dilute HCl (300 mL), and the mixture was extracted with toluene. The solvent was evaporated under reduced pressure, and the resulting solid was purified by column chromatography on silica gel (petrol ether/CH_2Cl_2, 3:1) to yield the yellow product (40 mg, 40%). Mp: 285 °C. ^{1}H NMR (300 MHz, $C_2D_2Cl_4$, 100 °C): δ 10.14 (s, 2H), 9.88 (s, 2H); 8.96 (s, 2H), 5.40 (sept, J = 5.9 Hz, 2H), 3.89 (t, J = 7.7 Hz, 4H), 2.47−2.36 (m, 4H), 2.23−2.18 (m, 4H), 2.09−2.02 (m, 4H), 1.71−1.66 (m, 4H), 1.48−1.21 (m, 64H), 0.87−0.76 (m, 18H). ^{13}C NMR (75 MHz, $C_2D_2Cl_4$, 100 °C, spin−echo experiment): δ 142.09 (C═O), 130.46 (t), 130.20 (q), 129.64 (q), 128.58 (t), 127.16 (q), 126.75 (t), 124.36 (q), 123.16 (q), 123.03 (q), 122.58 (q), 122.35 (q), 121.71 (q), 55.59 (CH), 34.06 (CH_2), 33.09 (CH_2), 32.04 (CH_2), 31.97 (CH_2), 31.70 (CH_2), 30.02 (CH_2), 29.77 (CH_2), 29.43 (CH_2), 29.34 (CH_2), 27.41 (CH_2), 22.76 (CH_2), 22.69 (CH_2), 14.13 (CH_3), 14.07 (CH_3). IR (KBr) υ (cm^{-1}): 2960, 2927, 2856, 1703, 1660, 1606, 1469, 1335, 926, 810. UV−vis ($CHCl_3$) λ_{max} (ϵ): 334 (70 000), 337 (70 000), 382 (8000), 404 (28 000), 429 (58 000), 477 (10 000), 511 nm (18 000 M^{-1} cm^{-1}). Fluorescence ($CHCl_3$) λ_{max}: 515, 555, 601 nm. MS (FD): [M^+] calcd for $C_{78}H_{110}N_2O_4$, 1139.76; found, 1139.8 (100%).

Scheme 2. Synthesis of 4[a]

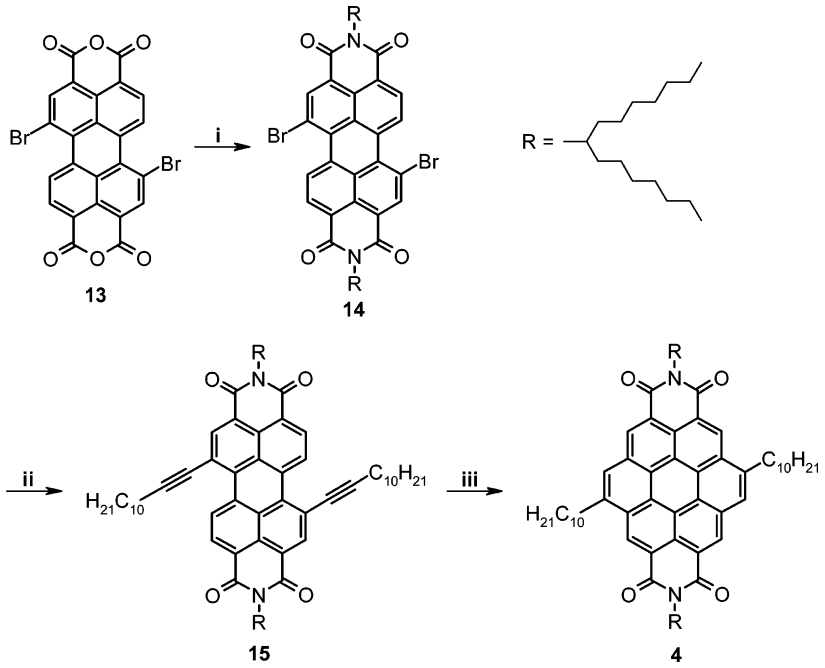

[a] (i) 1-Heptyloctylamine, NMP, 150 °C, 4 h, 39%; (ii) dodec-1-yne, triethylamine, THF, $[Pd(PPh_3)_2Cl_2]$, PPh_3, CuI, 80 °C, 16 h, 64%, and (iii) DBU, toluene, 110 °C, 20 h, 40%.

Results and Discussion

Synthesis. PDI **1** has been synthesized from the corresponding bisanhydride as described in the literature.[36] TDI **2** and QDI **3** were synthesized by our new synthetic route including the synthesis of a boronic ester, Suzuki cross-coupling reaction, and final cyclodehydrogenation (Scheme 1).

The monofunctionalized perylene dicarboxmonoimide **8** was the key intermediate in the synthesis of rylene tetracarboxdiimides **2** and **3**. The commercially available perylene-3,4-dicarboxanhydride (**5**) was condensed with 1-heptyloctylamine in quinoline using zinc acetate as the catalyst, giving **6** in a good yield of 83%. Selective bromination in the 9-position using bromine in acetic acid as the solvent and iodine as the catalyst led to **7**, which could be isolated in nearly quantitive yield. With bis(pinacolato)diboron and $PdCl_2$(dppf), **7** was converted into the corresponding boronic ester **8** in 78% yield. Suzuki cross-coupling of this building block with 4-bromonaphthalene dicarboximide **11**, which was synthesized by condensation of 4-bromonaphthaline-1,8-dicarboxanhydride **10** and 1-heptyloctylamine in ethylene glycol, gave the terrylene precursor **11** whereas reaction with 9-bromoperylene dicarboxmonoimide **7** led to the quaterrylene precursor **12**. Both could be isolated in good yields of 79 and 76%, respectively. In the final step the precursors **11** and **12** were cyclized using K_2CO_3 as the base in ethanolamine. After isolation and purification by column chromatography, **2** and **3** were obtained in high yields (**2**, 85%; **3**, 83%).

The CDI **4** was prepared similar to the published *n*-alkyl derivatives (Scheme 2).[35] 1,7-Dibromoperylene tetracarboxdianhydride **13** was first condensed with 1-heptyloctylamine in NMP yielding 39% of **14**, which than reacted with 1-dodec-1-yne under Hagihara conditions to form the coronene precursor **15** (64%). The final ring closing occurred at 110 °C using DBU as a strong but non-nucleophilic base giving **4** in 40% yield.

UV/Vis−Absorption Behavior. The absorption bands of the compounds **1**−**4** measured in chloroform are shown in Figure 2. The bathochromic shift of the absorption of TDI **2** and QDI **3** compared to that of PDI **1** is attributed to the extension of the core π-conjugated system by one and two naphthaline units, respectively. The absorption spectrum of PDI **1** is characterized by three absorption bands with maxima at 458, 489, and 526 nm with the typical perylene diimide fine structure. The maxima of the absorption spectra of TDI **2** are shifted by about 125 nm with respect to the PDI **1** and are located at 547, 598, and 651 nm. In line with expectations the absorption of QDI **3** is shifted even more bathochromically by about 111 nm compared with TDI **2**. The spectrum of QDI **3** has a strong absorption maximum at 762 nm and a shoulder in the region of 688 nm. The CDI **4** can be regarded as a perylene expanded along the short molecular axis. Its absorption spectrum shows three bands in the visible reagion: a weak band at 511 nm and two stronger bands at 337 and 429 nm causing the yellow color. The bands at 511 and 429 nm show the typical vibronic structure of a perylene. Semiempirical calculations could relate the absorption bands with the electronic transitions.[37] All dyes **1**−**4** show high molar extinction coefficients. The extinction coefficient increases within the homologous series of rylene tetracarboxdiimides from PDI **1** (ϵ = 90.000 M^{-1}

(36) Langhals, H.; Demmig, S.; Potrawa, T. *J. Prakt. Chem.* **1991**, *333*, 733.

(37) Calculations were done by Dr. P. Erk (BASF-AG) and are discussed in Schlichting, P. Ph.D. Thesis, University of Mainz, Mainz, Germany, 1998.

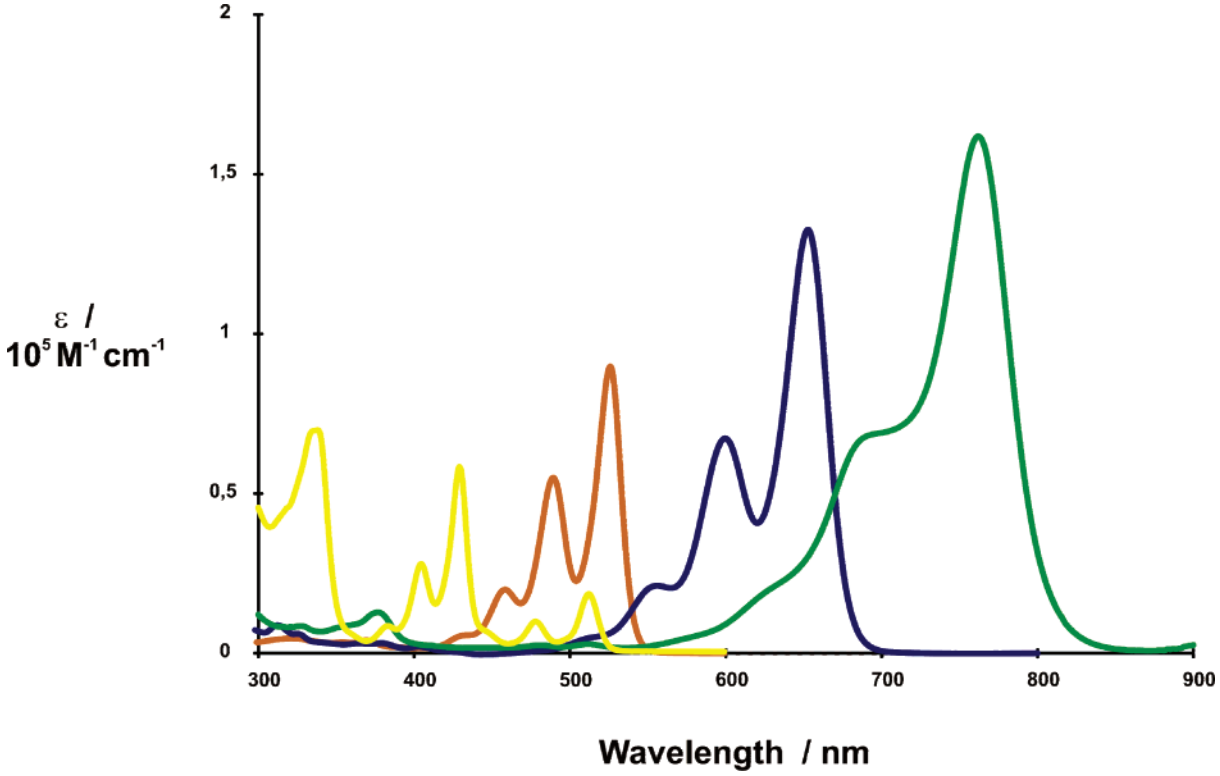

Figure 2. Absorption spectra of **4** (yellow line), **1** (orange line), **2** (blue line), and **3** (green line) in chloroform.

Table 1. Summary of the Thermal Behavior of the Investigated Compounds 1−4

sample	phase transition[a]	temperature, °C	enthalpy, kJ mol^{-1}
PDI **1**	C_r−I	130	18.82
TDI **2**	C_r−I	278	31.42
QDI **3**	Col_p−Col_{ho}	188	7.52
	Col_{ho}−I	>500	
CDI **4**	Col_p−I	285	17.64

[a] Abbreviations: C_r, crystalline phase; Col_p, plastic crystalline phase; Col_{ho}, columnar hexagonal ordered liquid crystalline; and I, isotropic.

cm^{-1}) over TDI **2** (ϵ = 127.000 M^{-1} cm^{-1}) to QDI **3** (ϵ = 162.000 M^{-1} cm^{-1}). CDI **4** has a molar extinction coefficient of 58.000 M^{-1} cm^{-1}.

Thermal Behavior. The thermal behavior was determined by using thermogravimetric analysis (TGA) and DSC, whereby the thermal data are summarized in Table 1. The phases were assigned on the basis of additional X-ray diffraction studies, which will be described in the next section. TGA indicated a pronounced thermal stability of all compounds **1**−**4** up to 450 °C, which is extremely high compared to other mesogens such as HBC.[38] The carboxylic imides incorporated into a six-membered ring are known to be stabilized by their very high resonance energy leading to a higher thermal stability of the molecules.[39] Figure 3 shows the DSC scans for all four derivatives upon heating. A strong dependence of the phase transition temperatures on the size of the aromatic core is obvious. At room temperature PDI **1** and TDI **2** were crystalline, whereby PDI **1** showed the lowest phase transition from the crystalline phase directly to the isotropic phase at 130 °C. With increasing core size

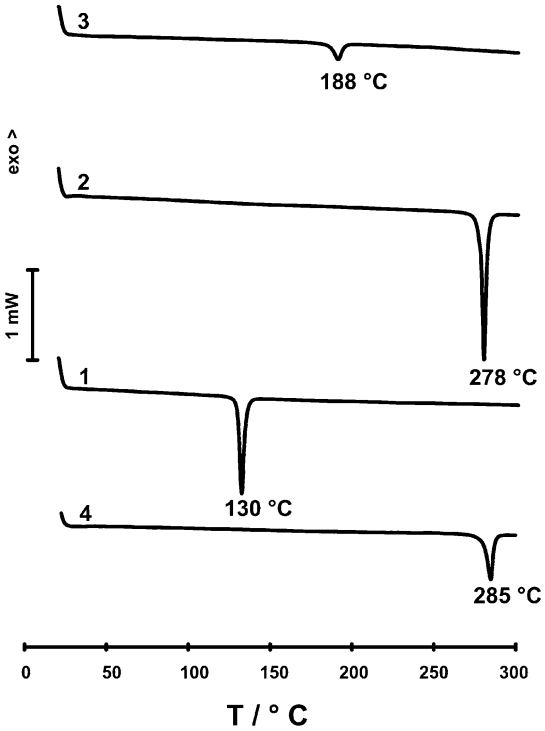

Figure 3. DSC traces of PDI **1**, TDI **2**, QDI **3**, and CDI **4** (heating rate of 10 K min^{-1}).

the isotropization temperature (T_i) was shifted to 278 °C for TDI **2**. To our knowledge, this is the first TDI derivative with an accessible isotropization temperature. In contrast to the first two derivatives, QDI **3** and CDI **4** were assigned as plastic crystalline. CDI **4** showed a transition at 285 °C, which is very similar to the corresponding value of the TDI **2**. This further illustrates the concept that the isotropization temperature is strongly related to the core size within this

(38) Gherghel, L.; Kübel, C.; Lieser, G.; Räder, H.-J.; Müllen, K. *J. Am. Chem. Soc.* **2002**, *124*, 13130.
(39) Langhals, H. *Heterocycles* **1995**, *40* (1), 477.

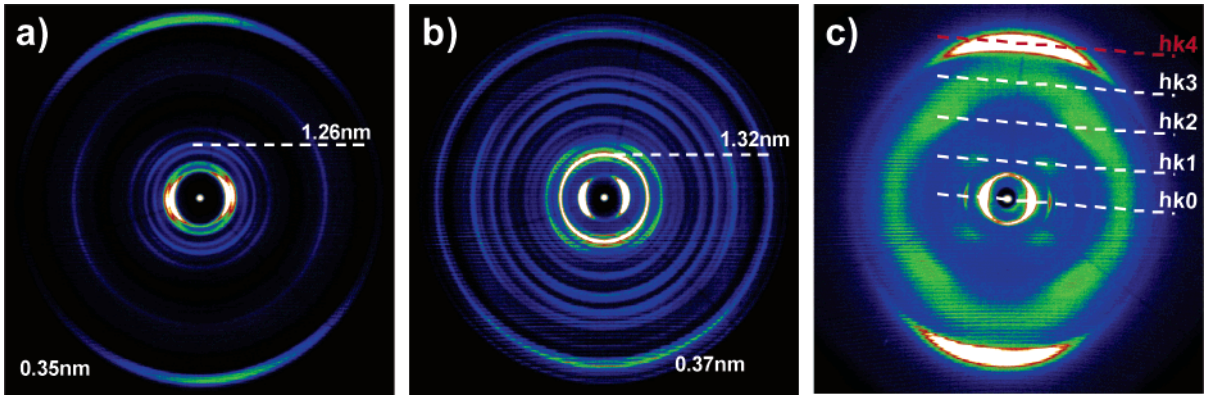

Figure 4. 2D-WAXS patterns of (a) PDI **1**, (b) TDI **2**, and (c) CDI **4** at room temperature. As an example, the reflections indicating the periodicity along the columnar structures are assigned by the Miller indices in the pattern of CDI **4**.

Table 2. Summary of the Structure Evaluation of the Investigated Compounds

sample	phase	2D lateral unit cell	packing parameters, nm
PDI **1**	C_r	Orthorhombic	$a = 1.67$ $b = 2.08$
TDI **2**	C_r	Hexagonal	$a = 2.94$
QDI **3**	Col_p	Hexagonal	$a = 3.09$
	Col_{ho}	Hexagonal	$a = 3.29$
CDI **4**	Col_p	Hexagonal	$a = 2.46$

homologous series of compounds. Additionally, QDI **3** revealed a liquid crystalline state at 188 °C which ranged above a temperature of 500 °C.

Structural Evaluation by X-ray Scattering. To investigate the supramolecular organization, the samples were prepared by filament extrusion using a home-built mini-extruder.[6] The compounds were mechanically aligned in their deformable state to ensure a sufficient orientation of the columns along the shearing direction. PDI **1**, TDI **2**, and CDI **4** were extruded about 130 °C below their isotropization temperatures, whereas QDI **3** was oriented in its mesophase. The samples were positioned vertically with respect to the 2D-WAXS detector.

Figure 4a,b depicts the room temperature 2D-WAXS patterns of PDI **1** and TDI **2**. In both cases, sharp and distinct equatorial reflections indicated well-aligned columnar structures along the extruded filaments. Furthermore, the positions of these reflections assigned a two-dimensional lateral unit cell which described the intercolumnar arrangement (summarized in Table 2). For PDI **1**, the two high-intensity equatorial reflections were fitted to an orthorhombic lattice with the parameters of $a = 1.67$ nm and $b = 2.08$ nm, whereas a hexagonal arrangement with $a = 2.94$ nm was found for TDI **2**. The appearance of multiple meridional reflections at similar positions in the patterns of PDI **1** and TDI **2** suggested an identical intracolumnar stacking of the molecules. Distinct wide-angle meridional reflections were related to the intracolumnar π -stacking period of 0.35 nm for PDI **1** and of 0.37 nm for TDI **2**. Thereby, the disks were orthogonally arranged with respect to the columnar axis. Additional meridional reflections corresponding to 1.26 nm (PDI **1**) and 1.32 nm (TDI **2**) implied also a correlation between every fifth disk within the stacks. Such organization was more evident for QDI **3** and CDI **4**, which could be extruded in a more plastic state, providing a more pronounced supramolecular alignment. The enhancement of the structure resulted in the appearance of more distinct reflections in the 2D-WAXS pattern, as shown in Figures 4c and 5.

Identical to the above-described packing of PDI **1** and TDI **2**, the high-intensity wide-angle meridional reflections in the patterns of QDI **3** and CDI **4** revealed the characteristic intracolumnar cofacial distance between 0.34 and 0.35 nm for both compounds with an orthogonal arrangement of the cores to the columnar axes. The relationship between the simple π-stacking distance and the additional middle-range meridional reflections, for instance, for QDI **3** 1.28 nm/0.34 nm $\sim$ 4, suggested for both cases an additional intracolumnar superperiodicity of every fifth molecule along the columns. This organization was induced by the rotation of each molecule by 45° to the adjacent disks attaining the initial lateral positional order after 180°. As illustrated schematically in Figure 6 for the rylene molecules, the great space demand of the bulky aliphatic side chains, branched very close to the aromatic core, might be one reason for the helical packing. It has been reported that intermolecular dipole−dipole interactions between the carbonyl groups of the imide are a major driving force which causes the rylene molecules to orient on average with a rotation between neighboring molecules.[27,40] In contrast, the introduction of different numbers of phenoxy substituents in the *bay* regions of the perylene core resulted in a longitudinal offset of the stacked molecules.[40] The helical arrangement was in agreement with the two-dimensional lateral hexagonal unit cell with the packing parameter of 3.09 nm for QDI **3** and 2.46 nm for CDI **4**, because the columns possessed a symmetric shape due to the helical stacking of the molecules as shown in Figure 6 for the top view. The large number of higher order equatorial reflections indicated a pronounced long-range organization of the QDI **3** columnar structures.

Upon heating QDI **3** to the mesophase, the supramolecular organization changed. The lateral hexagonal lattice remained identical with a slightly larger packing parameter of 3.29 nm. In contrast, the disappearance of most of the meridional reflections implied a transformation of the intracolumnar packing of the disks. The orthogonal order of the aromatic cores toward the columnar axes was still present in the mesophase, but the helical organization diminished. This was in accordance with other discotic species showing helical

(40) Würthner, F.; Thalacker, C.; Diele, S.; Tschierske C. *Chem.—Eur. J.* **2001**, *7*, 2245.

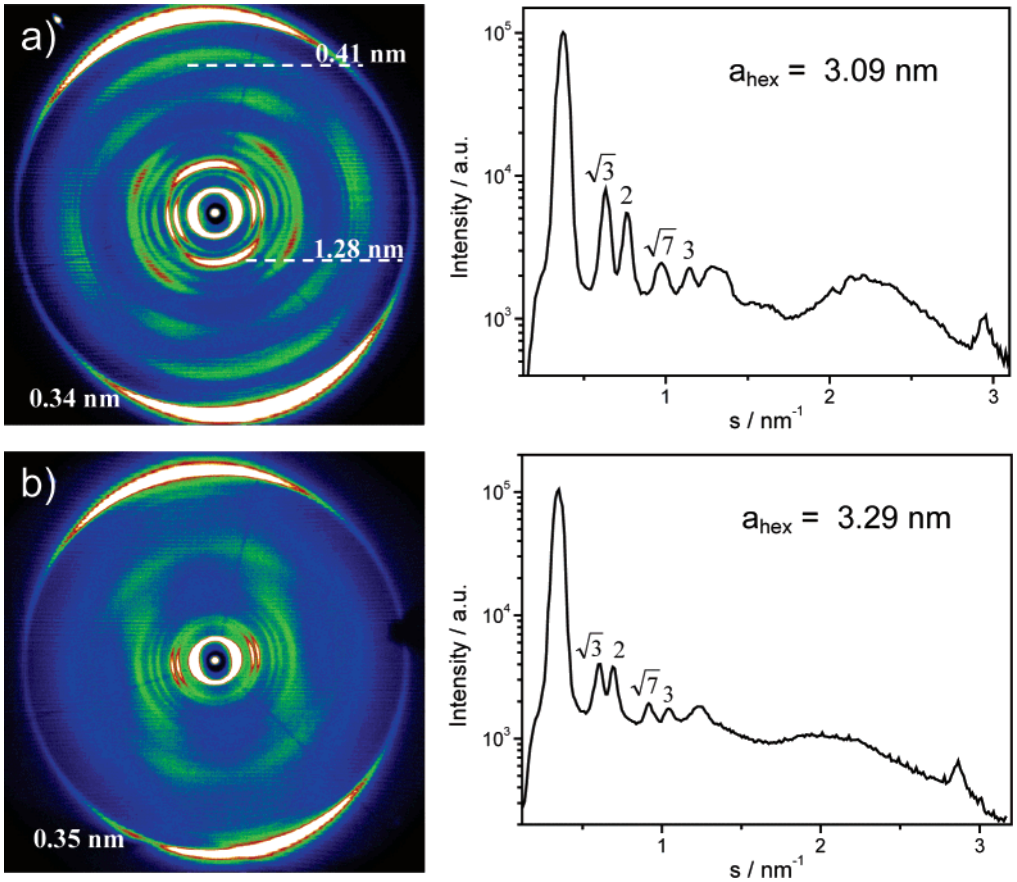

Figure 5. 2D-WAXS patterns and the equatorial scattering intensities as a function of the scattering vector of QDI **3** at (a) room temperature and (b) 200 °C.

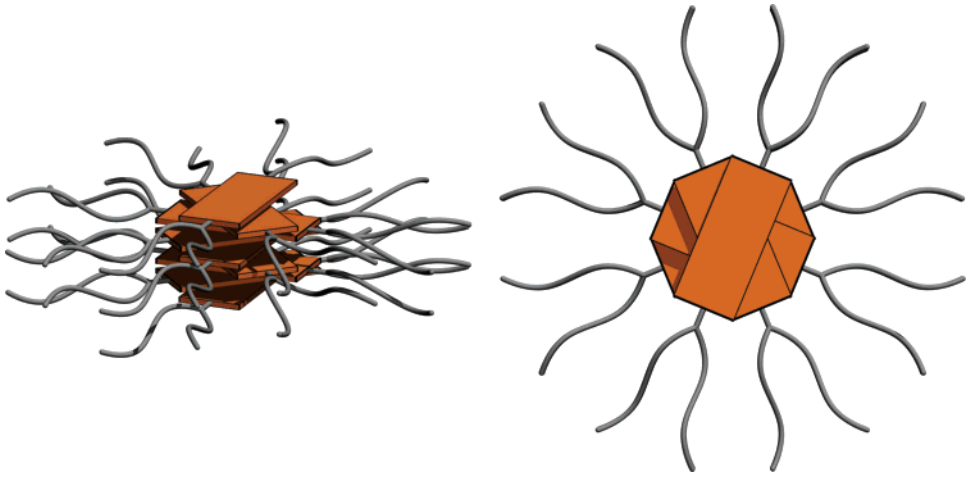

Figure 6. Schematic illustration of the intracolumnar packing of the rylene diimides **1**−**3**.

stacking only at ambient conditions.[41] In the liquid crystalline phase the molecular dynamics increased resulting in a longitudinal and lateral fluctuation of the disks within the stacks accompanied by an additional rotation around the columnar axes. But in this case, the diffuse and poor meridional reflections in the pattern in Figure 5b still implied a weak helical organization. When the sample was cooled back to room temperature the distinct helical arrangement in the plastic crystalline phase was recovered, proving the reversibility of the alternation of the structure at the phase transition.

Self-Organization from the Isotropic Phase. Remarkably enough, the accessible isotropization temperatures of PDI **1**, TDI **2**, and CDI **4** allowed a melt processing of the compounds and an investigation of their morphology after crystallization in regards to the different molecular designs. Because the substitution patterns of the rylenes and the coronene differed significantly, a distinction in the self-organization was expected. The materials were sandwiched between two glass slides and cooled from the isotropic phase.

(41) Wu, J. S.; Watson, M. D.; Zhang, L.; Wang, Z. H.; Müllen, K. *J. Am. Chem. Soc.* **2004**, *126*, 177.

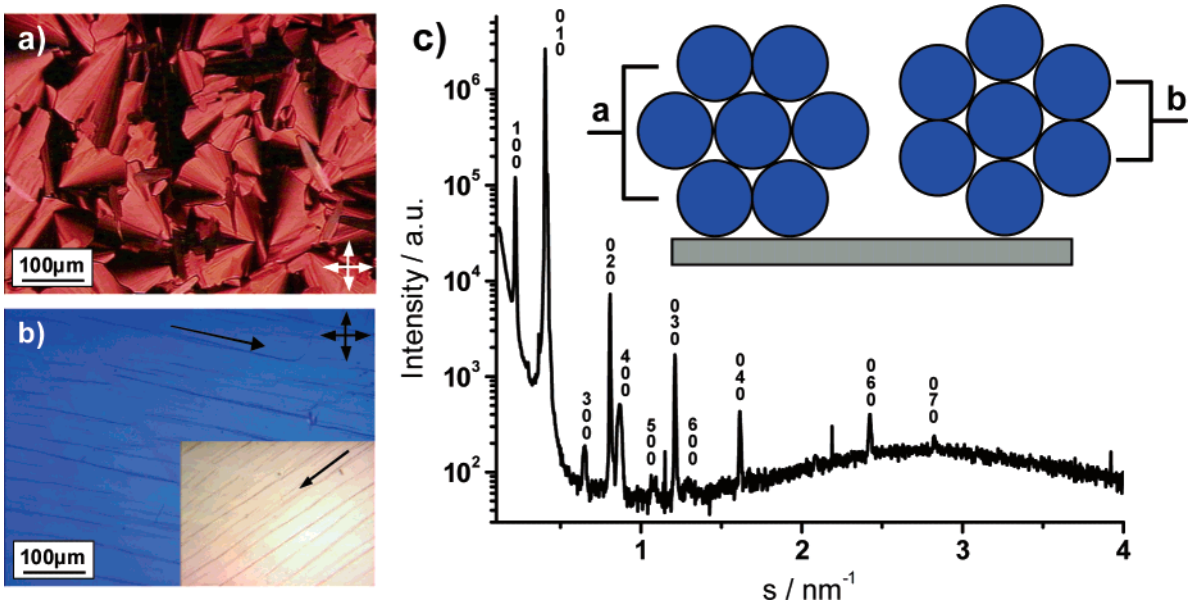

Figure 7. POM images of (a) PDI **1** and (b) TDI **2** cooled at 1 °C/min from the isotropic phase (inset in b, different orientation of the sample toward the polarized light; the arrows indicate the columnar alignment); (c) X-ray scattering in reflection of the film in part b (Miller indices are used to assign the reflections; the inset shows the two arrangements of the columns on the surface with $a = 4.4$ nm (corresponding to $h00$) and $b = 2.5$ nm (corresponding to $0k0$)).

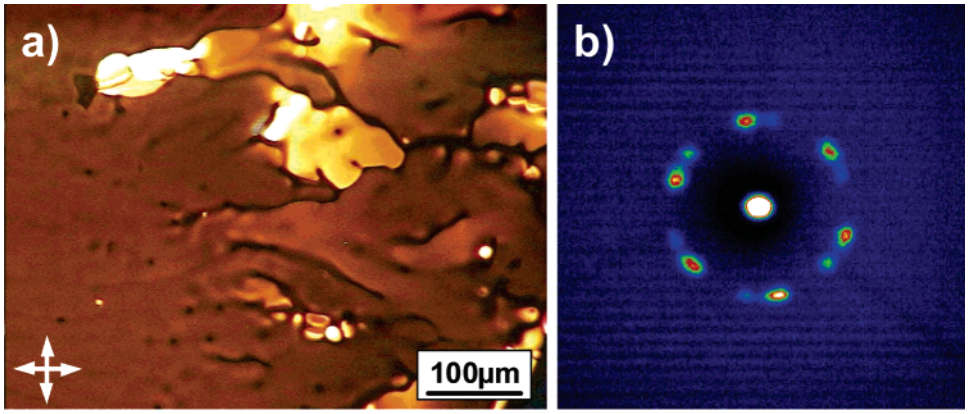

Figure 8. Thin film of CDI **4** aligned between two surfaces by cooling at a rate of 5 °C/min from the isotropic phase: (a) POM image and (b) 2D-WAXS pattern in transmission.

At room temperature, PDI **1** revealed optical textures with fan-shaped, relatively small domains (Figure 7a). The appearance of birefringence indicated defect structures with columns arranged predominately parallel to the surface, whereby the order was relatively poor.[42] In contrast, TDI **2** self-organized in large domains exceeding sizes of hundreds of micrometers. The birefringence and the high optical anisotropy suggested a pronounced uniaxial columnar alignment with edge-on arranged disks. To gain a deeper insight of the supramolecular organization of TDI **2**, large-area X-ray scattering in reflection was performed (Figure 7c). The appearance of a large number of sharp reflections confirmed that by slow cooling, TDI **2** self-organizes in domains of several hundred micrometers with high crystallinity of these films. The reflections were assigned only by the $h00$ and $0k0$ Miller indices indicating a particular arrangement of the columnar structure on the surface. The inset in Figure 7c illustrates schematically the two organizations with columns aligned parallel to the surface giving rise to only $h00$ and $0k0$ reflections. The two periods of 4.4 and 2.5 nm, derived from 100 and 010, were in good agreement with the hexagonal unit cell found for the extruded filament. The ratio of 4.4 nm/2.5 nm $\sim \sqrt{3}$ was characteristic for a hexagonal lattice with 2.53 nm as the packing parameter. It should be noted that this value was considerably smaller in comparison with the parameter found for the filaments, probably as a result of an enhanced packing of the side chains in the core periphery. To recapitulate, the X-ray scattering results confirmed the edge-on arrangement of the disks on the surface and the high columnar order by self-organization.

In contrast to the rylenes **1** and **2**, the CDI **4** molecules self-organized during cooling face-on leading to a homeotropic phase. Figure 8a shows a characteristic POM image of a homeotropically aligned thin film of CDI **4** with a texture displaying only negligible birefringence. A small number of defects, which were formed probably due to rapid cooling, led to minor birefringence in the image. A 2D-WAXS experiment in transmission gave the final proof for the

(42) Pisula, W.; Kastler, M.; Wasserfallen, D.; Robertson, J. W. F.; Nolde, F.; Kohl, C.; Müllen, K. *Angew. Chem., Int. Ed.* **2006**, *45*, 819.

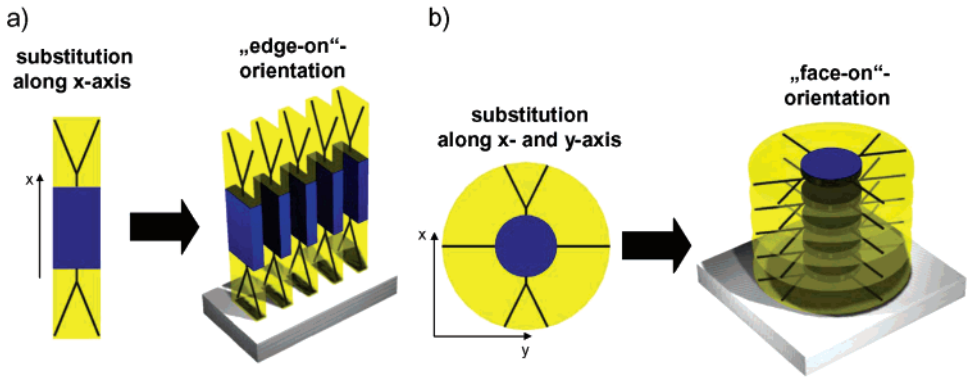

Figure 9. Schematic illustration of the arrangement of (a) the rylene diimides **1**−**3** and (b) the coronene diimide **4** on surfaces.

macroscopic orientation. The pattern in Figure 8b revealed a typical hexagonal reflection distribution indicating directly an alignment of the columns of CDI **4** in the direction of the incident beam and thus parallel to the surface normal. The packing parameter was slightly smaller as found for the mechanically aligned sample. The appearance of doubled reflections in the hexagonal pattern was explained as due to different domains, in which the hexagonal unit cells were just laterally displaced from each other, but the homeotropic alignment was maintained.

The different arrangements of the rylene and coronene molecules in the thin films sandwiched between two surfaces can be correlated with the molecular design of the disks (Figure 9). Despite the different shape and symmetry of the aromatic cores, one can derive from the above-mentioned results a strong influence of the substitution pattern of the core on the molecular self-orientation on a surface. The rylenes **1** and **2** were substituted at only two positions possessing a substitution pattern along one axis. Such molecules led to an edge-on arrangement, which seems to be the most favorable organization of these kinds of structures (Figure 9a). This is in accordance with the literature, where to our knowledge no disc-shaped molecules with substitution only in one direction revealing a homeotropic phase were reported. On the other hand, various uniformly substituted discotics in two dimensions were found to align homeotropically, as also in our case for CDI **4** (Figure 9b).[43,44] Although two different types of alkyl chains were attached to the CDI **4** disks, the alkyl mantle homogeneously surrounds the aromatic core. It seems that such a substitution pattern favors a face-on arrangement and leads to the homeotropic orientation.

Conclusions

The introduction of branched alkyl side chains and the variation of the aromatic core size of tetracarboxdiimides **1**−**4** allow a control of the UV absorption and the thermotropic behavior from rylene diimides. By varying the size of the π-conjugated system this series displays absorption maxima in the 430−760 nm region, which covers most of the visible part of the spectrum. Enlargement along the molecular long axis leads to bathochromic shifts, and extension along the short axis causes a hypsochromic shift. Concerning the thermotropic properties, this study revealed that, as expected, the phase transition temperatures increase with larger π-stacking areas of the aromatic cores, whereas the thermal stability is independent of the core size: all investigated compounds showed an identical high thermal stability. In contrast to the absorption behavior, the topology of the aromatic core has only little influence on the phase transition temperatures.

All four compounds showed columnar ordered structures with an intracolumnar superperiodicity of every fifth molecule along the columns. The comparison of the morphology after crystallization from the isotropic phase between PDI **1** and TDI **2** indicated that compounds consist of larger aromatic cores form bigger and better ordered domains. The first example of a meltable terrylene diimide derivative, TDI **2**, self-aligned over macroscopic dimensions with domains of several hundred micrometers with quasi "single-crystalline" ordering and edge-on arrangement of the molecules. This supramolecular organization on surfaces is beneficial for the implementation of these materials in field-effect transistors. In contrast, CDI **4** spontaneously self-assembled during cooling into a homeotropic alignment which is desired for photovoltaic cells. The different organizations of the molecules on surfaces were correlated with the uniformity of the alkyl substitution of the core. It can be generalized that irregularly substituted disk-shaped compounds can organize on surfaces upon cooling from the melt only in the edge-on manner.

This study contributes to the understanding of the complex organization mechanism of discotic molecules on surfaces, the control of which is essential for the implementation of these kinds of materials in electronic devices of different geometries.

Acknowledgment. Financial support from the Deutsche Forschungsgemeinschaft (Schwerpunkt organische Feldeffekttransistoren), BASF AG, and EU project NAIMO Integrated Project No. NMP4-CT-2004-500355 is gratefully acknowledged. S.M. thanks the "Fonds der chemischen Industrie" and the "Bundesministerium für Bildung und Forschung" for financial support.

CM060742C

(43) Pisula, W.; Tomovic, Z.; El Hamaoui, B.; Watson, M. D.; Pakula, T.; Müllen, K. *Adv. Funct. Mater.* **2005**, *15*, 893.
(44) Hatsusaka, K.; Ohta, K.; Yamamoto, I.; Shirai, H. *J. Mater. Chem.* **2001**, *11*, 423.